



ARTICLE

## Synthesis and Characterization of a Novel Bamboo Shaving Geopolymer Composite

Jiayu Zhang, Zhenyang Li and Xinli Zhang\*

College of Materials Science and Engineering, Central South University of Forestry and Technology, Changsha, 410004, China

\*Corresponding Author: Xinli Zhang. Email: xlzhang2011@yeah.net

Received: 20 September 2021 Accepted: 14 October 2021

### ABSTRACT

Geopolymers are inorganic aluminosilicate materials, which have been a great research interest as a material for sustainable development. However, they possess relatively low toughness properties similar to brittle solids. The limitation may be altered by fiber reinforcement to improve their strength and toughness. This research describes the synthesis of bamboo shaving (BS) reinforced geopolymer composites and the characterization of their mechanical properties. The effect of BS content (0–2 wt. %) on the physical and mechanical properties and microstructure of metakaolin based geopolymer paste were investigated. The workability, setting time, bulk density, apparent porosity, thermal conductivity, compressive strength, flexural strength, scanning electron microscopy (SEM), and X-ray diffraction (XRD) of geopolymer paste were determined. The results showed that the workability, setting time, density, and thermal conductivity decreased with the increasing of BS content. The BS content was proportional to the apparent porosity and a good linear relation was found between apparent porosity and BS content. The highest mechanical properties were achieved at an optimum BS content of 1.0 wt. %. The results of microstructural analysis revealed that BS act as inforging phase in matrix, reducing cracks and making a dense geopolymer, which leads to favorable adhesion of the composites and produces a geopolymer composite with better mechanical properties than that of pure geopolymer. However, when the BS content exceeded 1.0 wt. %, interfacial bonding between BS and geopolymer matrix became less. XRD analysis showed that BS has little effect on the mineral composition of metakaolin-based geopolymer and no new phase is formed.

### KEYWORDS

Bamboo shaving; geopolymer; strength; microstructure; thermal conductivity

### 1 Introduction

Geopolymers are now representing the most promising environmentally-friendly and sustainable alternative to ordinary Portland cement due to similar or even better bonding properties [1,2]. Geopolymers are synthesized by alkaline activation of aluminosilicates source materials (i.e., metakaolin, fly ash, slag, etc.) at ambient or slightly elevated temperatures [3], which have an amorphous 3D framework comprised by  $[AlO_4]$  and  $[SiO_4]$  tetrahedron. In the past three decades, geopolymers have attracted considerable attention, thanks to their proven high early strength, low shrinkage and permeability, low energy consumption and greenhouse gas emissions, and excellent corrosion and fire resistance behavior [4,5].



This work is licensed under a Creative Commons Attribution 4.0 International License, which permits unrestricted use, distribution, and reproduction in any medium, provided the original work is properly cited.

However, like Portland cement, geopolymers belong to quasi-brittle materials. The poor tensile and bending strengths can easily lead to catastrophic failure and represent the main drawback limiting the use of those materials in several applications [6,7]. Previous researches showed that the addition of micro- and macro-fibers into geopolymer matrix was considered currently one of the most effective solutions to enhance its toughness and decrease its brittleness [8]. Thus, the uses of carbon fiber [9], steel fiber [10], glass fiber [11], basalt fiber [12], and organic synthesized fibers [13,14] are most common for geopolymer composites.

Because of ever-increasing environment concern and the need to develop environment-friendly and energy-saving materials, natural fibers have been used as alternatives for steel or synthetic fibers as reinforcements in geopolymer composites in recent years. These include cotton, flax, jute, sisal, hemp, straw, pineapple leaf, wood and bamboo [15]. Natural fibers have special advantages over their synthetic counterparts, where the former represents a green and eco-friendly substitute, with lower density and cost, non-toxicity, ease of processing, renewability and biodegradability [16–20]. For example, the research reported by Sankar et al. [21] revealed that flexural strength and strain of geopolymer have been improved with 5 wt. % natural bamboo fiber reinforcement. Ribeiro et al. [22] evaluated the influence of alkali and water treatment of the bamboo fibers on the mechanical properties of the geopolymer composites. They found the compressive strength of bamboo reinforced geopolymer was lower than that of pure geopolymer.

However, after reviewing the previously published findings, no reference has been made to use of BS as reinforcement in geopolymer matrix up to date. Although bamboo fibers have been used to strengthen geopolymer, the effect of BS on geopolymer is even not known, little information is available on physical and mechanical properties, as well as microstructure changes of geopolymer. Therefore, the present study is devoted to determining the workability, setting time, bulk density, apparent porosity, thermal conductivity, compression strength, flexural strength, and microstructure development of geopolymer with BS as reinforcement.

## 2 Materials and Methods

### 2.1 Materials

Metakaolin (MK, 1250 mesh fineness) was the solid aluminosilicate source in the preparation of geopolymer matrix, obtained from Inner Mongolia, China. The chemical compositions of MK are shown in Table 1. Bamboo shaving (BS), which was obtained from a bamboo workshop (Yiyang, China) as residuals, was used in this study to explore the effect of the content on the physical and mechanical properties of the composites. The density of BS is 0.68 g/cm<sup>3</sup> and the moisture content is 5.89%. BS was not specially pretreated before being added to the geopolymer matrix. The main chemical constituents of BS were around 41 wt. % cellulose, 28 wt. % lignin and 10 wt. % hemicellulose. The micrographs of MK and BS were shown in Figs. 1 and 2, respectively.

**Table 1:** Chemical compositions of MK by mass (%)

Composition	SiO <sub>2</sub>	Al <sub>2</sub> O <sub>3</sub>	Fe <sub>2</sub> O <sub>3</sub>	TiO <sub>2</sub>	CaO	K <sub>2</sub> O	MgO	P <sub>2</sub> O <sub>5</sub>	Na <sub>2</sub> O	ZrO <sub>2</sub>	LOI
MK	50.13	42.55	3.41	2.40	0.45	0.35	0.17	0.15	0.15	0.11	0.13

The alkaline activator consisted of sodium silicate solution (water glass) and sodium hydroxide (NaOH). The water glass was purchased from Zhongfa Water Glass Factory in Foshan, China, which contained 26.5 wt. % SiO<sub>2</sub> and 8.3 wt. % Na<sub>2</sub>O (modulus Ms. = 3.3). Analytically pure agent NaOH was obtained from Sinopharm Chemical Reagents Shanghai Co. Ltd., China. The modulus was adjusted to 1.7 by dissolving solid NaOH in the water glass. The alkali activator solution was premixed and left to rest for 24 h at ambient temperature prior to casting.

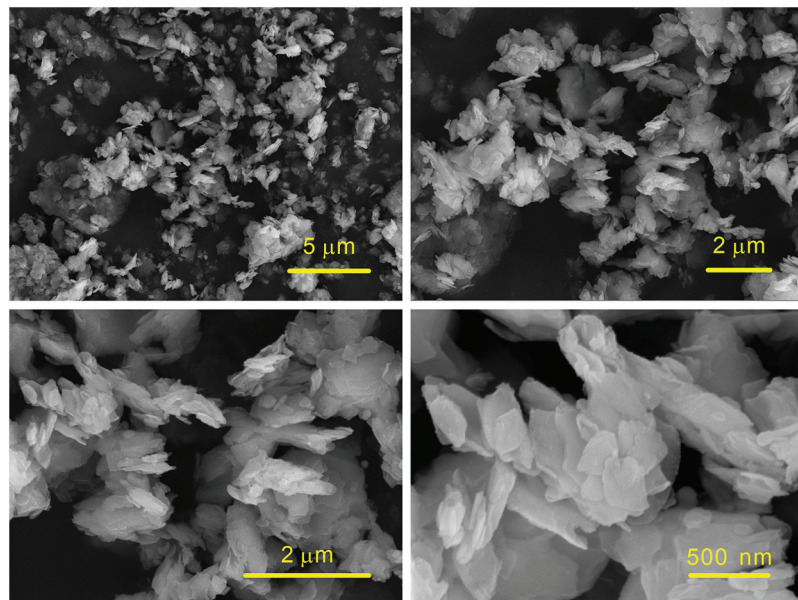


**Figure 1:** The micrographs of MK

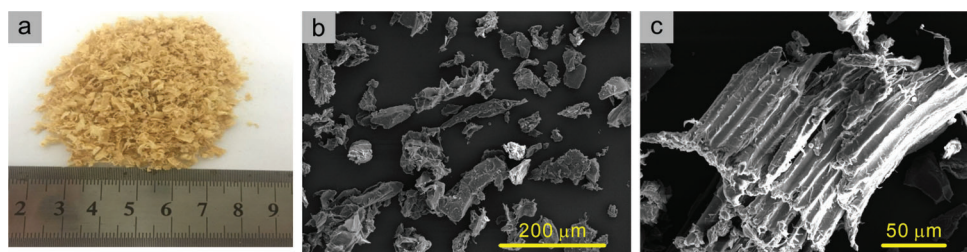


**Figure 2:** The morphology of bamboo shaving: macro morphology (a) and micrograph (b and c)

## 2.2 Mix Design and Specimen Preparation

To determine the effect of the BS on properties of MK based geopolymer, 5 specimens of geopolymer composites reinforced with 0, 0.5, 1, 1.5 and 2 wt. % BS were designed and prepared by alkaline activation of MK in sodium silicate solution. The details of geopolymer mixtures are given in [Table 2](#).

**Table 2:** Mix proportion design for geopolymer paste (mass, %)

Sample code	MK (g)	Alkaline activator (g)	BS content (wt. %)
BS0	100	120	0
BS0.5	100	120	0.5
BS1	100	120	1.0
BS1.5	100	120	1.5
BS2	100	120	2.0

MK and BS were mixed for 2 min before contacting with alkaline liquid activator, and then the mixture was slowly added into the activator solution and mixed for 5 min. The fresh paste was rapidly poured into the molds and vibrated for 3 min on the vibration table, then cured at room temperature for 24 h. In order to prevent the evaporation of water, polyethylene film was used to cover the specimen during the setting and hardening process. After demolding, all specimens were subjected to further curing in a standard condition ( $22 \pm 2^\circ\text{C}$ , and  $90 \pm 5\%$  relative humidity) up to acquired days for the research of properties and microstructure.

### **2.3 Performance Testing and Characterization**

#### **2.3.1 Flow Test and Setting Time**

The flow test for workability and the setting time were carried according to the Chinese standard GB/T 8077-2000 and GB/T 1346-2011, respectively. Both in these two tests, three specimens were tested and an average of measurements was taken.

#### **2.3.2 Bulk Density and Apparent Porosity**

The bulk density ( $D_b$ ) and apparent porosity ( $P_a$ ) were determined according to ASTM C20 and calculated using the Eqs. (1) and (2), respectively. Three specimens were tested and an average of measurements was taken.

$$D_b = \frac{m_0}{m_1 - m_2} \quad (1)$$

$$P_a = \frac{m_1 - m_0}{m_1 - m_2} \times 100\% \quad (2)$$

where  $m_0$  is the weight of the dried sample;  $m_1$  is the weight of the sample saturated in air; and  $m_2$  is the weight of the sample suspended in water.

#### **2.3.3 Thermal Conductivity**

The thermal conductivity test was performed on the  $200 \times 200 \times 40 \text{ mm}^3$  cubes according to ASTM D518. All specimens were first moist-cured for 28 days, and then air-dried for 14 days followed by oven drying at  $100 \pm 2^\circ\text{C}$  for 24 h.

#### **2.3.4 Compressive and Flexural Strength**

The strength tests were undertaken based on the Chinese standard GB/T 17671-1999. Cubic specimens were used in compressive strength tests ( $40 \times 40 \times 40 \text{ mm}^3$ ) and flexural strength tests ( $40 \times 40 \times 160 \text{ mm}^3$ ). The tests were performed by using an electronic universal testing machine (MWD-50, Jinan, China) with a loading speed of 2.4 kN/s and 50 N/s for the compressive and flexural tests, respectively. Six and three specimens were measured for compressive strength and flexural strength tests, respectively, and the average calculated.

#### **2.3.5 Micrographs Test**

The changes in microstructure and morphological of geopolymer composites as well as the nature of interactions between BS and matrix were studied using a TESCAN field emission scanning electronic microscopy (SEM) at an accelerating voltage of 10 kV for photomicrographs.

#### **2.3.6 XRD Analysis**

The X-ray diffraction (XRD) analysis was determined by an EmpyreanX-ray diffractometer (PANalytical, Netherlands) equipped with monochromatic Cu-K $\alpha$  radiation at 36 kV and 20 mA. A typical scan is from 10 to  $80^\circ$  with a scan speed of  $0.02^\circ/\text{s}$ .

### 3 Results and Discussion

#### 3.1 Workability and Setting Time

In order to check the physical consistency of fresh geopolymer mix with and without BS, the workability of geopolymer composites blended with different BS content was measured, the flow diameter measured results were shown in Fig. 3a. For geopolymer mix without BS (BS0), the workability value is 158 mm. While the workability value for BS0.5, BS1, BS1.5, and BS2 are 156, 149, 140 mm, and 136 mm, respectively. The trend of workability in Fig. 3a shows the workability values are gradually decreased as the increasing content of BS from BS0 to BS2. This may be caused by the hindrance which is provided by BS to the free flow and the water absorption of BS with a porous structure as depicted in Fig. 2.

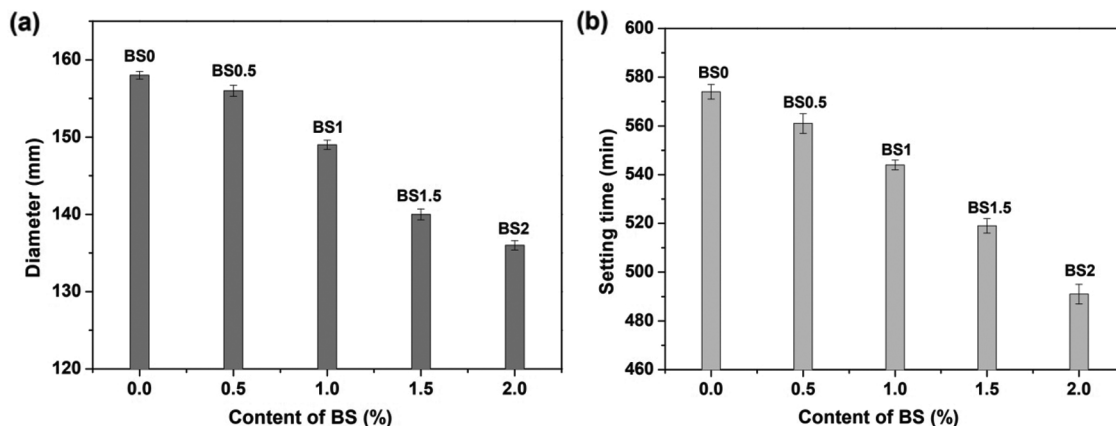


**Figure 3:** Relationship between flow diameter and the BS content in geopolymer (a), and Relationship between setting time and the BS content in geopolymer (b)

The test results of setting time were shown in Fig. 3b, it can be found that the setting time decreases with the increase of BS content. Compared with BS0, BS1 and BS2 reduced the setting time by 5.23% and 14.46%, respectively. BS has a water absorbent property, which makes the composite more viscous and hardens faster, so the addition of BS accelerates the solidification process of geopolymer.

#### 3.2 Bulk Density and Apparent Porosity

The effect of BS content on bulk density of geopolymer composites is shown in Fig. 4a. The bulk densities of BS0, BS0.5, BS1, BS1.5, and BS2 at 28 days were 1.67, 1.66, 1.64, 1.63, and 1.62 g/cm<sup>3</sup>, respectively. The results showed that the density of geopolymer reinforced with BS decreased with BS content increasing. As shown in Fig. 4a, it can be found that a good linear relation between the bulk density and BS content. Similar results have also been reported by Duan et al. [23] who found that the density of sawdust reinforced geopolymer composites decreased with sawdust content increasing.

Fig. 4b shows the test results of apparent porosity of geopolymer pastes. The apparent porosity of BS0, BS0.5, BS1, BS1.5, and BS2 at 28 days was 28.74, 29.13, 29.75, 30.06, and 30.4%, respectively. Compared to that of BS0, the increases were approximately 1.36, 3.51, 4.59, and 5.78%. It indicates that BS content is proportional to apparent porosity. These results are similar to the reported by Alomayri et al. [24], who found the porosity increases with increasing in weight percent of cotton fibers.

The addition of BS increases the apparent porosity, but not significantly. The reason is that the metakaolin based geopolymer itself has certain porosity, and the porosity brought by BS acts as the internal pores of the original geopolymer.

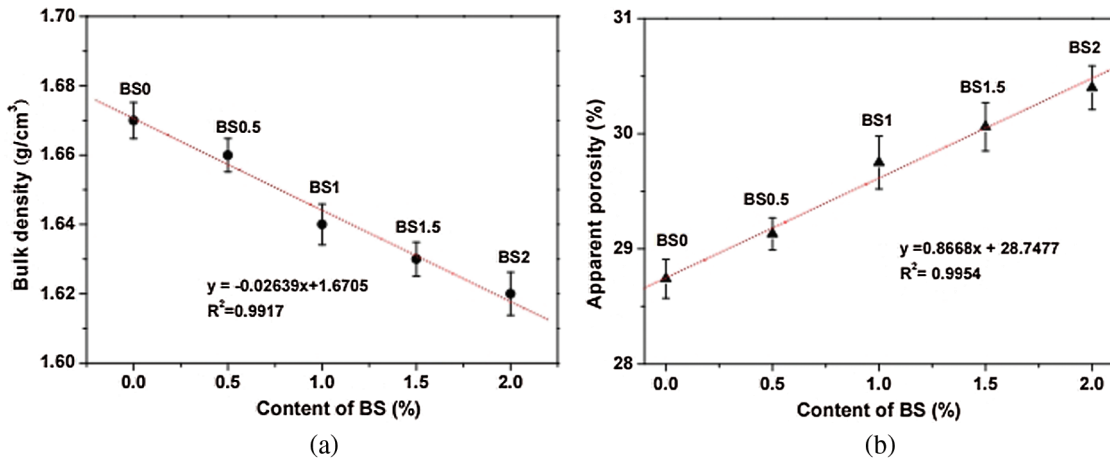


**Figure 4:** Relationship between bulk density and the BS content in geopolymer (a), and Relationship between apparent porosity and the BS content in geopolymer (b)

### 3.3 Thermal Conductivity

As shown in Fig. 5, the thermal conductivity of BS0, BS0.5, BS1, BS1.5, and BS2 at 28 days was 0.133, 0.124, 0.103, 0.099, and 0.095  $\text{W}/(\text{m}\cdot\text{K})$ , respectively. These are comparable to that of expanded perlite (0.101–0.134  $\text{W}/(\text{m}\cdot\text{K})$ ) and have a good insulation performance. The thermal conductivity of BS reinforced geopolymer decreases with the increase of BS content. The reductions in thermal conductivity were 6.8%–28.6%, which related to the porous cellular structure and low density of BS.

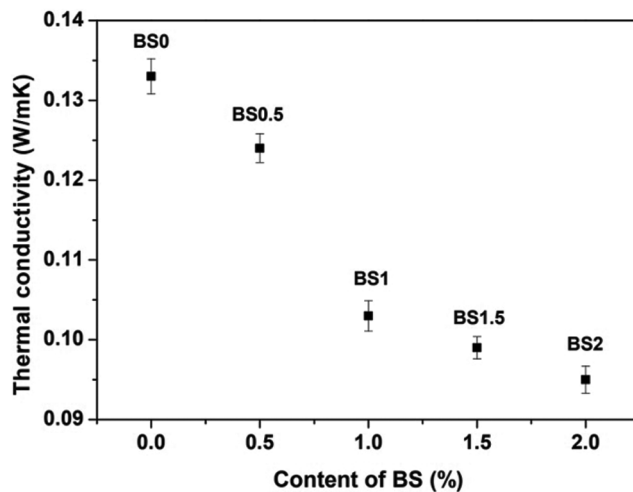


**Figure 5:** Relationship between thermal conductivity and the BS content in geopolymer

### 3.4 Compressive Strength

Compressive strength tests of geopolymer specimens were performed on each mixture at 3, 7, and 28 days of curing. The results were shown in Fig. 6. Compared with BS0, the compressive strength of geopolymers containing different BS content was improved at three different curing periods, and the compressive strength of BS1 was the highest. The compressive strengths of BS1 at 3, 7, and 28 days of curing were increased by 8.20%, 12.15%, and 7.76% compared with the pure geopolymer (BS0), respectively.

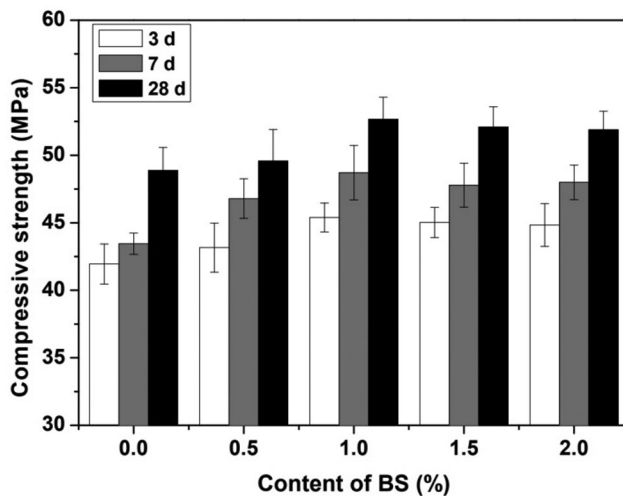


**Figure 6:** The compressive strength of geopolymers with different content of BS

However, the compressive strengths of BS1.5 and BS2 decrease slightly. The reason for the reduction in compressive strength with the addition of higher content of BS may be attributed to these BS agglomeration together and leaving voids in the matrix. Other reasons for the reduction may be that BS is easy to absorb water and it has absorbed too much water, reducing the geopolymer around the BS enough water required for geopolymerization, which in turn decreased the adhesion between BS and the matrix.

The change trend of the compressive strength in this work is in agreement with the research results by other researchers. For example, Alomayri et al. [25] investigated the compressive strength of cotton fiber-reinforced geopolymer, they found the geopolymer composites with 0.5% cotton fibers had the highest compressive strength. Similar trend was also reported by Li et al. [26] for hemp fiber-reinforced concrete.

### 3.5 Flexural Strength

The results of flexural strength were presented in Fig. 7. It can be seen that the flexural strength of geopolymer composites was higher than that of neat geopolymer, and BS1 has the highest flexural strength for all the geopolymer samples regardless of curing ages. The flexural strengths of BS1 at 3, 7, and 28 days of curing were increased by 10.76%, 7.25%, and 7.04% compared with the pure geopolymer (BS0), respectively. The enhancement in flexural strength could be due to a good dispersion of BS at the optimum content in the geopolymer matrix which helps to increase the adhesion or interaction at the interface of matrix and BS. Therefore, the stress is transferred from the matrix to the BS, BS is pulled out from the matrix, thus delaying the growth of micro-cracks and increasing the flexural strength.

However, further increasing of the BS content induces poor workability and the non-homogeneity within the matrix such that agglomerations are formed which degrade the interfacial bonding between BS and the matrix. These flaws may act as stress concentrators to cause the reductions in flexural strength. Similar trend was also reported by other researchers. For instance, the research reported by Alomayri et al. [27] showed the flexural strength improves slightly when the cotton fiber content is lower than 2.1%, and continuously decreases when the content is greater than this value. Chen et al. [28–30] also reported that the highest flexural strength was obtained by adding 2% natural fibers into geopolymer matrix.

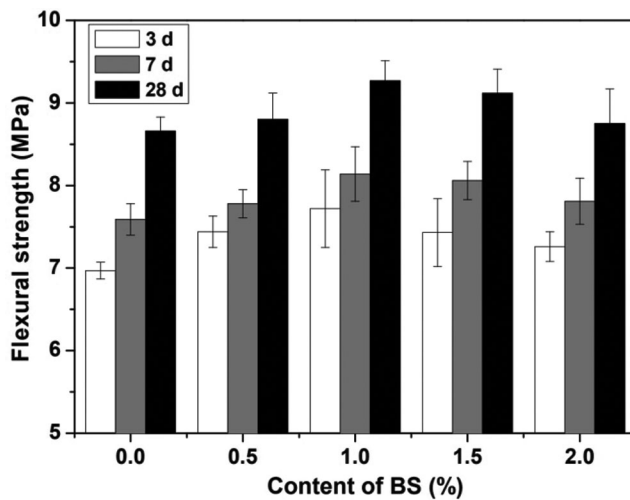


**Figure 7:** The flexural strength of geopolymer with different content of BS

### 3.6 Interface Topography Analysis

In this composite system, geopolymer played a binder role and BS a reinforcing role. The bonding between BS and matrix is primarily important to obtain a strong geopolymer and serves as the proof of BS reinforced geopolymer. Therefore, the influence mechanism of BS on the properties of geopolymer composites was explored by SEM to identify the fracture surface and internal microstructure.

The morphological changes of reference geopolymer (BS0) and geopolymer specimens with addition of 1% and 2% BS (BS1 and BS2) after 28 days of curing were selected to assess the effects of BS and were presented in Fig. 8. The SEM of geopolymer paste without BS (Fig. 8a) shows some pores and cracks. With the increasing of the BS, compact matrix of BS1 shown in Fig. 8b can be found compared to BS0. A denser structure of BS2 was also observed when compared to BS0 (Fig. 8c).

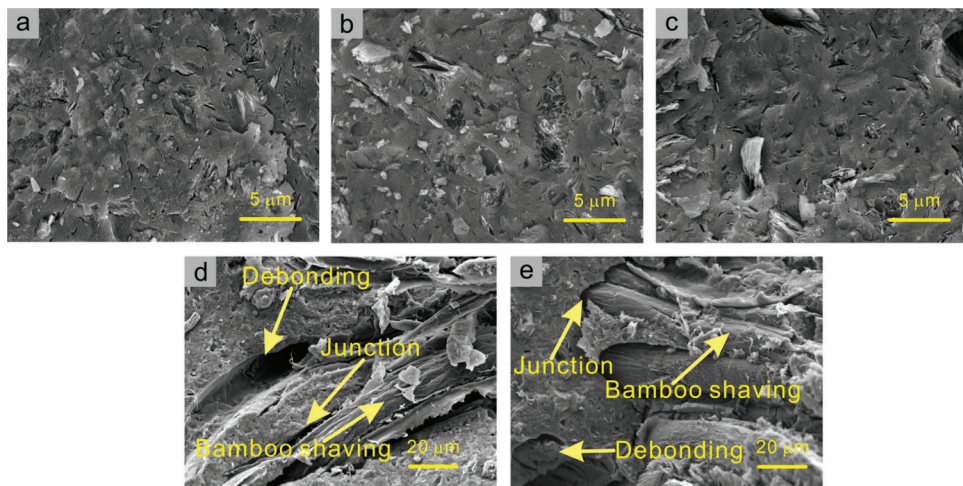


**Figure 8:** The morphological changes of geopolymer with different content of BS. Fracture surface of BS0 (a); fracture surface of BS1 (b); fracture surface of BS2 (c); bonding interface between BS and matrix for BS1 (d); and bonding interface between BS and matrix for BS2 (e)

However, higher BS content will result in the aggregation of BS and increase the pores of geopolymer matrix. Compared with BS2 (Fig. 8e), there were smaller cracks at the junction interface of BS and geopolymer for BS1 (Fig. 8d), which indicated that BS1 had better interface bonding. A good adhesion between the BS and the matrix with some debonding was observed along the BS end (Figs. 8d and 8e), which is evidently noticeable that BS fracture and pull-out are the main mechanisms that lead to the enhanced compressive and flexural strength.

On the basis of the results of strength as tested above, it can be concluded that mechanical properties of geopolymer are closely related to the micro cracks development and the interfacial adhesion between BS and geopolymer matrix.

### 3.7 Phase Analysis

In order to study the effect of BS on the crystalline phase of geopolymer paste, BS0, BS1, and BS2 were selected to be characterized by XRD. The XRD patterns of the geopolymer specimens are shown in Fig. 9, a broad hump at  $2\theta = 20\text{--}40^\circ$  can be found, which is typical for the amorphous phase of geopolymer consisting of randomly orientated Si-Al tetrahedral. It shows that the XRD patterns of samples with different BS content were similar, indicating that the addition of BS did not promote another polymerization product and did not significantly alter the degree of amorphous and crystallization.

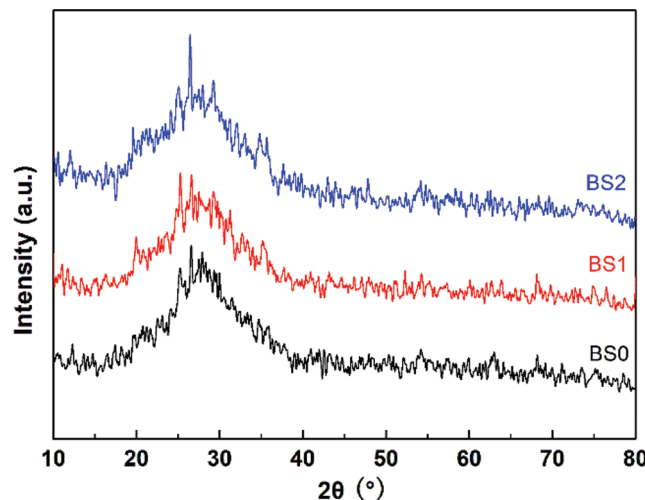


**Figure 9:** XRD patterns of geopolymer with different content of BS

## 4 Conclusions

The experimental results from this study are summarized below:

- (1) BS has a cellular porous structure according to the SEM. Therefore, BS addition decreases the workability, setting time, and bulk density of geopolymer, and a good linear relation was found between bulk density and BS content.
- (2) The apparent porosity of BS reinforced geopolymer increases with the BS content. This results in the decrease in thermal conductivity of material and thus improves the thermal performance.
- (3) The compressive strength and flexural strength of geopolymer composites were significantly improved with the use of BS and 1% BS content provided the optimum improvement.

(4) The analysis results of mechanical properties are consistent with those of microstructure. The good mechanical properties of composites are closely related to their dense structure and good interfacial adhesion. It is believed that BS is feasible to be used as reinforcing component in geopolymers.

**Funding Statement:** This work was supported by the Excellent Youth Foundation of Education Department of Hunan Province, China (20B612) and Changsha Natural Science Foundation of China (kq2014158).

**Conflicts of Interest:** The authors declare that they have no conflicts of interest to report regarding the present study.

## References

- Pacheco-Torgal, F., Castro-Gomes, J., Jalali, S. (2008). Alkali-activated binders: A review. Part 2. About materials and binders manufacture. *Construction and Building Materials*, 22(7), 1315–1322. DOI 10.1016/j.conbuildmat.2007.03.019.
- Shi, C. J., Fernández-Jiménez, A., Palomo, A. (2011). New cements for the 21st century: The pursuit of an alternative to Portland cement. *Cement and Concrete Research*, 41(7), 750–763. DOI 10.1016/j.cemconres.2011.03.016.
- Mackenzie, K. J. D., Welter, M. (2014). Geopolymer (aluminosilicate) composites: Synthesis, properties and applications. In: Low, I. M., *Advances in ceramic matrix composites (Second Edition)*, pp. 445–470. UK: Woodhead Publishing Limited. DOI 10.1533/9780857098825.3.445.
- Duxson, P., Fernández-Jiménez, A., Provis, J. L., Lukey, G. C., Palomo, A. et al. (2007). Geopolymer technology: The current state of the art. *Journal of Materials Science*, 42(9), 2917–2933. DOI 10.1007/s10853-006-0637-z.
- Yang, K. H., Song, J. K., Song, K. I. (2013). Assessment of CO<sub>2</sub> reduction of alkali-activated concrete. *Journal of Cleaner Products*, 39(9), 265–272. DOI 10.1016/j.jclepro.2012.08.001.
- Sarker, P. K., Kelly, S., Yao, Z. T. (2014). Effect of fire exposure on cracking, spalling and residual strength of fly ash geopolymer concrete. *Materials & Design*, 63(6), 584–592. DOI 10.1016/j.matdes.2014.06.059.
- Dias, D. P., Thaumaturgo, C. (2005). Fracture toughness of geopolymeric concretes reinforced with basalt fibers. *Cement and Concrete Composites*, 27(1), 49–54. DOI 10.1016/j.cemconcomp.2004.02.044.
- Nematollahi, B., Sanjayan, J., Shaikh, F. U. A. (2016). Matrix design of strain hardening fiber reinforced engineered geopolymer composite. *Composites Part B: Engineering*, 89(8), 253–265. DOI 10.1016/j.compositesb.2015.11.039.
- Lin, T. S., Jia, D. C., Wang, M. R., He, P. G., Liang, D. F. (2009). Effects of fibre content on mechanical properties and fracture behaviour of short carbon fibre reinforced geopolymer matrix composites. *Bulletin of Materials Science*, 32(1), 77–81. DOI 10.1007/s12034-009-0011-2.
- Bernal, S., Gutierrez, R. D., Delvasto, S., Rodriguez, E. (2010). Performance of an alkali-activated slag concrete reinforced with steel fibers. *Construction and Building Materials*, 24(2), 208–214. DOI 10.1016/j.conbuildmat.2007.10.027.
- Alomayri, T. (2017). The microstructural and mechanical properties of geopolymer composites containing glass microfibres. *Ceramics International*, 43(5), 4576–4582. DOI 10.1016/j.ceramint.2016.12.118.
- Timakul, P., Rattanaprasit, W., Aungkavattana, P. (2016). Improving compressive strength of fly ash-based geopolymer composites by basalt fibers addition. *Ceramics International*, 42(5), 6288–6295. DOI 10.1016/j.ceramint.2016.01.014.
- Rickard, W. D. A., Vickers, L., Riessen, A. V. (2013). Performance of fibre reinforced, low density metakaolin geopolymers under simulated fire conditions. *Applied Clay Science*, 73, 71–77. DOI 10.1016/j.clay.2012.10.006.
- Choi, S. J., Choi, J. I., Song, J. K., Lee, B. Y. (2015). Rheological and mechanical properties of fiber-reinforced alkali-activated composite. *Construction and Building Materials*, 96(6), 112–118. DOI 10.1016/j.conbuildmat.2015.07.182.

15. Silva, G., Kim, S., Aguilar, R., Nakamatsu, J. (2020). Natural fibers as reinforcement additives for geopolymers—A review of potential eco-friendly applications to the construction industry. *Sustainable Materials and Technologies*, 23(16), e00132. DOI 10.1016/j.susmat.2019.e00132.
16. Kornienko, K., Fraczek, E., Pytlak, E., Adamski, M. (2016). Mechanical properties of geopolymer composites reinforced with natural fibers. *Procedia Engineering*, 151, 388–393. DOI 10.1016/j.proeng.2016.07.395.
17. Yan, L. B., Kasal, B., Huang, L. (2016). A review of recent research on the use of cellulosic fibres, their fibre fabric reinforced cementitious, geo-polymer and polymer composites in civil engineering. *Composites Part B: Engineering*, 92(3), 94–132. DOI 10.1016/j.compositesb.2016.02.002.
18. Rodríguez-Félix, F., Del-Toro-Sánchez, C. L., Tapia-Hernández, J. A. (2020). A new design for obtaining of white zein micro- and nanoparticles powder: Antisolvent-dialysis method. *Food Science and Biotechnology*, 29(5), 619–629. DOI 10.1007/s10068-019-00702-9.
19. Rodríguez-Félix, F., López-Cota, A. G., Moreno-Vásquez, M. J., Graciano-Verdugo, A. Z., Quintero-Reyes, I. E. et al. (2021). Sustainable-green synthesis of silver nanoparticles using safflower (*Carthamus tinctorius* L.) waste extract and its antibacterial activity. *Heliyon*, 7(4), e06923. DOI 10.1016/j.heliyon.2021.e06923.
20. Del-Toro-Sánchez, C. L., Rodríguez-Félix, F., Cinco-Moroyoqui, F. J., Juárez, J., Ruiz-Cruz, S. et al. (2021). Recovery of phytochemical from three safflower (*Carthamus tinctorius* L.) by-products: Antioxidant properties, protective effect of human erythrocytes and profile by UPLC-DAD-MS. *Journal of Food Processing and Preservation*, 45(9), 1209. DOI 10.1111/jfpp.15765.
21. Sankar, K., Sá Ribeiro, R. A., Sá Ribeiro, M. G., Kriven, W. M. (2017). Potassium-based geopolymer composites reinforced with chopped bamboo fibers. *Journal of the American Ceramic Society*, 100(1), 49–55. DOI 10.1111/jace.14783.
22. Sá Ribeiro, R. A., Sá Ribeiro, M. G., Sankar, K., Kriven, W. M. (2016). Geopolymer-bamboo composites—A novel sustainable construction material. *Construction and Building Materials*, 123(8), 501–507. DOI 10.1016/j.conbuildmat.2016.07.037.
23. Duan, P., Yan, C. J., Zhou, W., Luo, W. J. (2016). Fresh properties, mechanical strength and microstructure of fly ash geopolymer paste reinforced with sawdust. *Construction and Building Materials*, 111(7), 600–610. DOI 10.1016/j.conbuildmat.2016.02.091.
24. Alomayri, T., Shaikh, F. U. A., Low, I. M. (2013). Characterisation of cotton fibre-reinforced geopolymer composites. *Composites Part B: Engineering*, 50(9), 1–6. DOI 10.1016/j.compositesb.2013.01.013.
25. Alomayri, T., Low, I. M. (2018). Synthesis and characterization of mechanical properties in cotton fiber-reinforced geopolymer composites. *Journal of Asian Ceramic Societies*, 1(1), 30–34. DOI 10.1016/j.jascer.2013.01.002.
26. Li, Z. J., Wang, L. J., Wang, X. G. (2004). Compressive and flexural properties of hemp fiber reinforced concrete. *Fibers and Polymers*, 5(3), 187–197. DOI 10.1007/BF02902998.
27. Alomayri, T., Shaikh, F. U. A., Low, I. M. (2013). Thermal and mechanical properties of cotton fabric-reinforced geopolymer composites. *Journal of Materials Science*, 48(19), 6746–6752. DOI 10.1007/s10853-013-7479-2.
28. Chen, R., Ahmari, S., Zhang, L. Y. (2014). Utilization of sweet sorghum fiber to reinforce fly ash-based geopolymer. *Journal of Materials Science*, 49(6), 2548–2558. DOI 10.1007/s10853-013-7950-0.
29. Kroehong, W., Jaturapitakkul, C., Pothisiri, T., Chindaprasirt, P. (2018). Effect of oil palm fiber content on the physical and mechanical properties and microstructure of high-calcium fly ash geopolymer paste. *Arabian Journal for Science and Engineering*, 43(10), 5215–5224. DOI 10.1007/s13369-017-3059-0.
30. Taveri, G., Bernardo, E., Dlouhy, I. (2018). Mechanical performance of glass-based geopolymer matrix composites reinforced with cellulose fibers. *Materials*, 11(12), 2395. DOI 10.3390/ma11122395.